Development 135, 3425-3434 (2008) doi:10.1242/dev.012237

Eya4 regulation of Na^+/K^+-ATPase is required for sensory system development in zebrafish

Libin Wang[1,2], William F. Sewell[3], Sang D. Kim[1], Jordan T. Shin[4], Calum A. MacRae[4], Leonard I. Zon[2,5], J. G. Seidman[1,2,*] and Christine E. Seidman[1,2,*,†]

To investigate the mechanisms by which mutations in the human transcriptional co-activator *EYA4* gene cause sensorineural hearing loss that can occur in association with dilated cardiomyopathy, we studied *eya4* expression during zebrafish development and characterized *eya4* deficiency. *eya4* morphant fish embryos had reduced numbers of hair cells in the otic vesicle and lateral line neuromasts with impaired sensory responses. Analyses of candidate genes that are known to be expressed in a temporal and spatial pattern comparable to *eya4* focused our analyses on *atp1b2b*, which encodes the β2b subunit of the zebrafish Na^+/K^+-ATPase. We demonstrate *atp1b2b* levels are reduced in *eya4* morphant fish and that morpholino oligonucleotides targeting the *atp1b2b* gene recapitulated the *eya4* deficiency phenotypes, including heart failure, decreased sensory hair cell numbers in the otic vesicle and neuromasts, and abnormal sensory responses. Furthermore, *atp1b2b* overexpression rescued these phenotypes in *eya4* morphant fish. We conclude that *eya4* regulation of Na^+/K^+-ATPase is crucial for the development of mechanosensory cells and the maintenance of cardiac function in zebrafish.

KEY WORDS: Eya4, Na^+/K^+-ATPase, Hair cells, Myocardium, Neuromast, Otic vesicle

INTRODUCTION

Eya molecules are evolutionarily conserved transcriptional co-activators that participate in the development of multiple organs, including the eye, pituitary gland, muscle, kidney, inner ear and heart (Hanson, 2001; Kawakami et al., 2000; Rebay et al., 2005; Schonberger et al., 2005). Eya proteins contain a highly conserved carboxyl domain with phosphatase activity and interaction sites for Sine oculis (Six) proteins, and a variable amino domain with unknown functions (Hanson, 2001; Kawakami et al., 2000; Rebay et al., 2005; Schonberger et al., 2005). Interactions with Six proteins permit Eya proteins to translocate into the nucleus (Hanson, 2001; Rebay et al., 2005) where phosphatase activity releases transcriptional repression caused by Six-Dachshund and other molecules (Li et al., 2003; Rayapureddi et al., 2003; Tootle et al., 2003). Human deletions in *EYA4* cause a dominant form of sensorineural hearing loss (Pfister et al., 2002; Wayne et al., 2001), which sometimes is accompanied by late-onset dilated cardiomyopathy (Schonberger et al., 2000; Schonberger et al., 2005). The gene targets regulated by Eya4, Six and Dachshund in the ear or heart are unknown.

Na^+/K^+-ATPases comprise a plasma membrane enzymatic complex that regulates ion homeostasis in many eukaryotic tissues (Blanco and Mercer, 1998; Therien and Blostein, 2000). With ATP hydrolysis, the complex extrudes three Na^+ ions and imports two K^+ ions, therein establishing a chemical and electrical gradient. Na^+/K^+-ATPase participates in maintaining the delicate balance of high K^+, low Na^+ in the endolymphatic fluid that bathes the sensory epithelium in the membranous labyrinth of the inner ear and that is required for sensory transduction (Wangemann, 2002). In the heart, Na^+/K^+-ATPase cooperates with the Na^+/Ca^{2+} exchanger to produce inotropic effects on myocytes (Ingwall and Balschi, 2006; Schwinger et al., 2003). Heart failure is commonly treated with cardiac glycosides (e.g. digitalis), which bind the α subunit of the Na^+/K^+-ATPase and inhibit pump functioning so that intracellular Na^+ increases, Ca^{2+} extrusion decreases and contractile performance is enhanced (Ingwall and Balschi, 2006; Schwinger et al., 2003).

The heterodimeric Na^+/K^+-ATPases complexes contain a catalytic α subunit and a stabilizing β subunit (Jorgensen, 1974); both are required for enzyme activity (Goldin, 1977; Horowitz et al., 1990). There is considerable evolutionary diversity in the subunit isoforms of Na^+/K^+-ATPases. Human and rodent genomes contain four α subunit and three β subunit isoforms, while the zebrafish (*Danio rerio*) genome encodes nine α and six β isoforms (Blasiole et al., 2002; Levenson, 1994; Malik et al., 1998; Rajarao et al., 2002; Rajarao et al., 2001; Shamraj and Lingrel, 1994; Underhill et al., 1999). Isoform expression is spatially and temporally regulated (Peters et al., 2001). In human, rat and mouse, β2 subunit expression encoded by the *Atp1b2* gene is restricted to the marginal cells of the stria vascularis in the cochlea (Peters et al., 2001; Wangemann, 2002). Zebrafish have two β2 subunit genes: *atp1b2a* is expressed in the brain, spinal cord neurons and lateral line ganglia; *atp1b2b* predominates in the retina, neuromasts and otic vesicles (Rajarao et al., 2002). *atp1b2b* gene expression is required for otic vesicle development and otolith formation (Blasiole et al., 2006).

Na^+/K^+-ATPases are also essential for zebrafish heart development. Two zebrafish mutants, *heart and mind* (Shu et al., 2003) and *small heart* (Yuan and Joseph, 2004), are caused by deficiency of *atp1a1a.1* (also known as *atp1α1B1*) and have malformed hearts (due to defective primitive heart tube extension and cardiomyocyte differentiation) with reduced contractility and heart rate.

We characterized *eya4* expression in the mechanosensory epithelia of the zebrafish otic vesicle and in neuromasts, sensory patches that are related to the mammalian inner ear (Whitfield et al., 1996; Whitfield et al., 2002), and demonstrated that *eya4* antisense morpholino oligonucleotides reduced hair cell numbers in these

[1]Harvard Medical School, Department of Genetics and [2]Howard Hughes Medical Institute, 77 Avenue Louis Pasteur, Boston, MA 02115, USA. [3]Department of Otolaryngology and Program in Neuroscience, Harvard Medical School and MEEI, Boston, MA 02114, USA. [4]Developmental Biology Laboratory and Cardiovascular Research Center, Massachusetts General Hospital, Charlestown, MA 02129, USA. [5]Stem Cell Program and Division of Hematology/Oncology, Children's Hospital Boston and Dana-Farber Cancer Institute, 300 Longwood Avenue, Boston, MA 02115, USA.

*These authors contributed equally to this work
†Author for correspondence (e-mail: cseidman@genetics.med.harvard.edu)

Accepted 13 August 2008

organs. Hypothesizing that Eya4 regulated the expression of Na^+/K^+-ATPase, we examined subunit levels in *eya4* morphant zebrafish and demonstrated the selective reduction of two subunits. Re-expression of the Na^+/K^+-ATPase β2b subunit rescued *eya4* deficiency in morphant zebrafish. Taken together, these results indicate that Eya4 regulates Na^+/K^+-ATPase, and therein provides a mechanism by which human *EYA4* mutations cause both hearing loss and heart disease.

MATERIALS AND METHODS

Zebrafish strain and maintenance

Zebrafish studies were reviewed and approved by the Institutional Animal Care and Use Committee (IACUC). Wild-type AB zebrafish were maintained, and embryos collected and staged, as previously described (Westerfield, 2000). Embryos were anesthetized with 0.16 mg/ml Tricaine (Sigma) in E3 solution prior to sacrifice.

In situ hybridization

Whole-mount in situ hybridization was performed as described (Jowett, 1999). Sections were hybridized with slight modifications (Schonberger et al., 2005). Zebrafish embryos were fixed with 4% paraformaldehyde (PFA) in phosphate buffered saline (PBS), embedded in paraffin, and longitudinally sectioned to view the otic vesicle and heart. Using full-length *eya4* and *atp1b2b* cDNAs as templates, RNA probes were synthesized and labeled using digoxigenin (DIG) RNA labeling kit (Roche). Isotope-labeled RNA probes were synthesized with ^{35}S-ATP and ^{35}S-UTP; signal was detected using liquid film emulsion autoradiography (Kodak) of Toluidine Blue-counterstained tissues.

Otic vesicle and neuromast analyses

All analyses were performed with the observers blinded to the morpholino oligonucleotide treatment status of the zebrafish embryos.

Phalloidin stains

Zebrafish embryos were fixed in methanol-free, 4% PFA in PBS buffer for 24-48 hours (4°C), washed in PBST (PBS with 0.5% Tween-20), and permeabilized either by incubation in 1% Triton X-100 in PBS (7 hours) or by incubation in acetone –15°C (20 minutes). After washing in PBST, embryos were reacted (2.5 hours) with 50 ng/ml FITC or Alexa Fluor 488-labeled phalloidin in 1% Triton X-100/PBS. After washing three times with PBST (30 minutes) embryos were embedded in agar or 50% glycerol and visualized using a Leica TCS SP2 confocal microscope.

DASPEI stains

Neuromast hair cells were stained with vital dye, 1 mM DASPEI [4-(4-(diethylamino)-styryl)-N-methylpyridinium iodide] (Molecular Probes) in E3 solution (5 mM NaCl, 0.17 mM KCl, 0.33 mM $CaCl_2$, 0.33 mM $MgSO_4$), for 10 minutes, then rinsed five times with E3 solution (Whitfield et al., 1996). Embryos were anaesthetized with 0.02% Tricaine in E3 solution and observed using a FM-1-43 filter set (Chroma).

Acridine Orange stains

Cell death was assessed by Acridine Orange staining (2 μg/ml) of zebrafish embryos as previously described (Blasiole et al., 2006). The otic vesicles were observed under a Zeiss Discovery V8 fluorescence dissecting microscope.

Otic vesicle morphology

A three-dimensional otic vesicle surface model was reconstructed from serial confocal images of the otic vesicle acquired by differential interference contrast imaging using the Amira Advanced 3D Visualization and Volume Modeling Software (Version 4.1.2, Mercury Computer Systems).

RNA isolation, RT-PCR and semi-quantitative PCR

Total RNA was isolated using Trizol Reagent (Invitrogen). RT-PCR and semi-quantitative RT-PCR reactions were carried out using One-Step RT-PCR kits (Qiagen), following the manufacturer's instructions (Ausubel et al., 2008). For semi-quantitative RT-PCR, 1 μg of total RNA was used as template where *eya1* and *atp1b2b* cDNA were co-amplified for 25 cycles in a 50 μl reaction using 0.3 μM of each of the gene-specific primers (*eya1*, 5′ATGGAAATGCAGGATCTAGCTAGT3′ and 5′CTGCTGCTCATTGGCTCTGTTTTAA3′; *atp1b2b*, 5′TGAGCGCACATTTAGTCCAG3′ and 5′GCACCACACGTGACATAAGG3′). Reactions (10 μl) were resolved on 2% agarose gels and band intensity was calculated using ImageJ software (NIH).

atp1b2b mRNA synthesis

Full-length *atp1b2b* cDNA was amplified from total RNA extracted from zebrafish embryos (72 hpf) by RT-PCR using the primer set 5′GCACGAGGTCTCTCTCTCTCTCTCTCC3′ and 5′AAAAAAAAAACAAACACTCTTGTCTGTTCAATCTCTGG3′; cDNA was then cloned into pCS2+ between the *Eco*RI and *Xho*I sites. The cloned sequence was verified. *atp1b2b* mRNA was subsequently synthesized using the mMESSAGE mMACHINE High Yield Capped RNA Transcription Kit (Ambion).

Morpholino oligonucleotides

All morpholino oligonucleotides were complimentary to splice donor sites and were injected into 1- to 2-cell-stage zebrafish embryos. Sequences and injected amounts of morpholino oligonucleotides against *eya4* (see also Schonberger et al., 2005) and against *atp1b2b* (denoted β2b) are provided below. Numbers denote the exon-intron splice donor sites targeted by the morpholino (e.g. MO3 indicates that the morpholino target is the splicing donor site at exon 3). Mismatch morpholinos (e.g. MO3mis) differ from the related morpholino oligonucleotides at five bases.

MO3eya4 (1 ng), TACTGATGTTACCTGTTGTCTACTG;
MO10eya4 (1 ng), TAATATGTATACCTGGCATCTGATA;
MO3mis (1 ng), TAATGATTTTAACTGTTCTCTAATG;
MO10mis (1 ng), TATTATCTATAGCTGGGATCTCATA;
MO1β2b (2.5 ng), AGCTAGTCTTACCCCAACTGCTCGC; and
MO4β2b (0.6 ng), TGTTTCTCATCTTACACGGTTGAGC.

Heart phenotypes

Observers who were blinded to the morpholino oligonucleotide treatment status of the zebrafish embryos assessed heart phenotypes. Cardiac dimensions and contraction cycle lengths (to deduce heart rate) were measured using quantitative high-speed image analysis as described (Schonberger et al., 2005).

Cardiac expression of *atp1b2b* was assessed using the pEGFP-N1 plasmid (Invitrogen). In brief, a 2.5-kb promoter fragment of the *atp1b2b* gene was cloned into pEGFP-N1. The modified plasmid (100 pg; denoted pβ2bprom) was injected into one-cell-stage embryos and fluorescence was examined daily using a Zeiss Discovery V8 microscope.

Startle reflex

Individual wild-type or morphant fish (72 hpf) with normal head morphology and tails that were not curved ventrally or dorsally were placed in a 100 mm Petri dish filled with 25 ml E3 solution. Startle reflexes were evoked by a single tap to a petri dish, with simultaneous video recording of movements. Zebrafish that moved outside of the camera field via coordinated swimming were scored as normal (see Movie 3 in the supplementary material). Zebrafish that either did not swim or moved only in concentric tight circles were scored as abnormal (see Movie 4 in the supplementary material). Startle reflexes were evoked at least three times in each zebrafish.

Statistics

Student's *t*-tests were used to compare hair cells in wild-type and morphant fish. Fisher exact tests were used to compare cardiac phenotypes and startle reflexes in wild-type and morphant fish. *P*-values <0.05 were considered significant. Means±standard error (s.e.m.) are reported.

RESULTS

Developmental expression of *eya4* in the otic vesicle

Previous studies (Schonberger et al., 2005) demonstrated that adult zebrafish express *eya4* in the otic vesicle and neuromast sensory organs. To characterize developmental expression, we studied

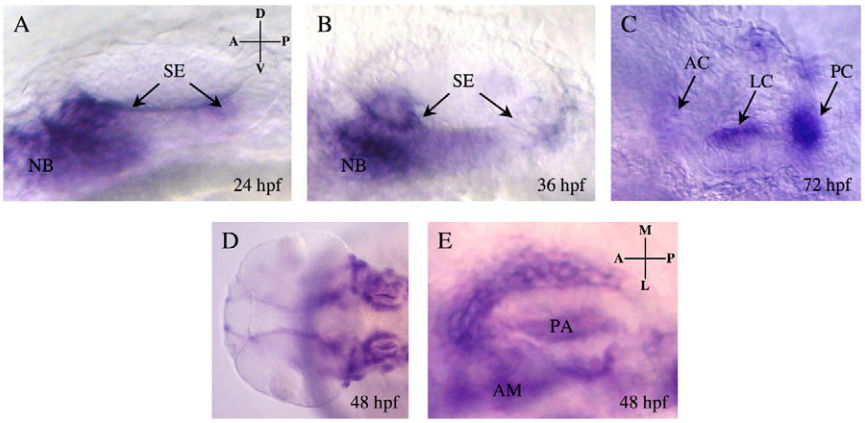

Fig. 1. *eya4* expression during otic vesicle development. Wild-type embryos were hybridized to DIG-labeled *eya4* antisense RNA probes. Lateral (**A-C**) and dorsal (**E**) views of single otic vesicles; (**D**) dorsal view of two otic vesicles. *eya4* signal (arrows) at 24 hpf (A) and 36 hpf (B) demarcated the developing sensory epithelia (SE) and neuroblast (NB). At 72 hpf (C), expression was maintained in the anterior, lateral and posterior cristae (AC, LC and PC, respectively) of the sensory epithelia. At 48 hpf (D,E), *eya4* signal was more diffuse within the otic vesicle and was prominent in the anterior macula (AM) and pharyngeal arch (PA; E). Background signal with *eya4* sense RNA probe was minimal (data not shown). D, dorsal; V, ventral; A, anterior; P, posterior; M, medial; L, lateral.

zebrafish embryos and tissue sections of the developing otic vesicle using *eya4* antisense probes. By 14 hours post-fertilization (hpf), *eya4* transcripts were detected at two distinct sites in the otic placode region (see Fig. S1A in the supplementary material). This pattern persisted through further otic placode development assessed at 16 and 18 hpf (see Fig. S1B,C in the supplementary material). At 18 hpf, an additional cluster of cells, anterior to the otic placode, which may give rise to ganglion neuroblasts (see below), also expressed *eya4* (see Fig. S1C in the supplementary material). By 24 hpf, *eya4* expression was most prominent along the anterior and posterior axis of the ventral side of the otic vesicle (Fig. 1A; see also Fig. S1D in the supplementary material), from where the progenitors of sensory epithelial cells originate (Whitfield, 2002; Whitfield et al., 2002). Neuroblasts in the statoacoustic ganglion, adjacent to the otic vesicle, also expressed *eya4* (Fig. 1A; see also Fig. S1D in the supplementary material). At 36 hpf this expression pattern was maintained, albeit with some broadening of ventral *eya4* expression (Fig. 1B). By 48 hpf, *eya4* expression was diffuse, and included the anterior macula (Fig. 1D,E) and pharyngeal arches (Fig. 1D,E), as well as several ganglia adjacent to the otic vesicle (Fig. 1D). *eya4* expression patterns in the otic vesicles were similar at 60 and 72 hpf (Fig. 1C; see also Fig. S1E; data not shown): *eya4* expression was restricted to the sensory patches (including hair cells and supporting cells) in the three cristae (anterior, lateral and posterior; see Fig. 1C, and Fig. S1E in the supplementary material) and in the two maculae (anterior and posterior; see Fig. S1E in the supplementary material; data not shown).

Impaired otic vesicle morphology in *eya4* morphant fish

To consider *eya4* roles in otic vesicle maturation, we examined the developmental effects of two *eya4* antisense morpholino oligonucleotides (MO3eya4 and MO10eya4), which are complementary to the splice donor sites of exon 3 and exon 10, respectively, in over 200 zebrafish embryos. Previous analyses using these morpholino oligonucleotides showed selective attenuation of *eya4* expression without changing *eya1* expression (Schonberger et al., 2005). Although maturation of the zebrafish otic vesicle is not complete until 120 hpf (Whitfield, 2002; Whitfield et al., 2002), analyses later than 72 hpf were not performed because morpholino oligonucleotides were diluted at these later developmental stages.

By acquiring differential interference contrast and serial confocal images of zebrafish otic vesicles at 72 hpf, we produced three-dimensional reconstructions of the otic vesicles (Fig. 2; see also Movies 1, 2 in the supplementary material). At 72 hpf, *eya4* morphant fish had smaller (cf. Fig. 2A and 2B) and misshaped (compare the DIC images of Fig. 3B-D) otic vesicles compared with wild-type embryos.

By 72 hpf, wild-type fish develop projections of epithelial pillars that grow and fuse in the center of the otic vesicle to provide scaffolding and to shape the developing semicircular canals (anterior, lateral and posterior), and each canal is associated with a corresponding crista (Whitfield et al., 2002) (see Fig. 2A, Fig. 3A,B; see also Movie 1 in the supplementary material). In *eya4* morphant embryos, the smaller-sized otic vesicle contained foreshortened, misshaped and, usually, disconnected epithelial pillar protrusions, so that portioning of the otic vesicle failed to occur (Fig. 2B, Fig. 3C,D; see also Movie 2 in the supplementary material). This led to malformed semicircular canals and the disruption of their association with the diminutive sensory cristae in *eya4* morphant fish (Fig. 2B, Fig. 3C,D; see also Movie 2 in the supplementary material).

The formation of otoliths (crystalline deposits of calcium carbonate and protein that are visible by light microscopy within otic vesicles) appeared unaffected in *eya4* morphant fish. Mismatch morpholino oligonucleotides against *eya4* (MO3mis and MO10mis) did not affect otic vesicle development (data not shown) in more than 100 zebrafish.

eya4 in sensory hair cell development

Sensory hair cell development in the otic vesicle was assessed by fluorescence-labeled phalloidin at 72 hpf. Staining of wild-type embryos (n=10) revealed five to seven delicate actin-rich stereocilia of hair cells projecting into each ampulla from the underlying anterior, lateral and posterior cristae (Fig. 4A), and an average of 38.3±0.9 hair cells in the anterior macula (n=6). Hair cells in the posterior macula were not assessed due to different imaging depths. Embryos treated with MO3mis or MO10mis had normal hair cell numbers (data not shown). By contrast, fluorescence labeled-phalloidin staining of *eya4* morphant fish (n=13) showed few or no stereocilia on cristae (anterior cristae, n=1.7±0.7; lateral cristae, n=1.4±0.6; posterior cristae, n=1.3±0.4; Fig. 4B), and fewer hair cells in the anterior macula (n=24.5±2.5; P≤0.0013).

To determine whether reduced hair cell numbers in *eya4* morphants reflected death of these specialized cells, we stained zebrafish embryos (n>15, each genotype) with Acridine Orange at 24 and 48 hpf (see Fig. S2 in the supplementary material). At 24 hpf, most otic vesicles from wild-type embryos had few if any Acridine Orange-stained cells. The average numbers of stained cells per otic vesicle were 0.2±0.6 (24 hpf) and 0.4±1.2 (48 hpf). In *eya4*

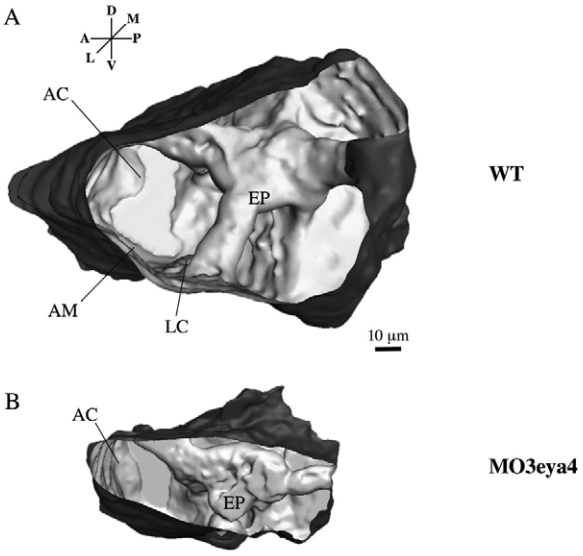

Fig. 2. Three-dimensional reconstruction of the zebrafish otic vesicle (72 hpf) generated from confocal images. (**A**) The otic vesicle of the wild-type zebrafish has well-formed epithelial pillars (EP) that shape the semicircular canals. The anterior cristae (AC), lateral cristae (LC) and anterior maculae (AM) are indicated. (**B**) The otic vesicle of an *eya4* morphant fish is smaller and misshapened, with fused epithelial pillars and malformed semicircular canals.

morphant fish, there were comparable average numbers of stained cells per otic vesicle: 0.3±0.7 (24 hpf; P=0.9 versus wild type) and 0.1±0.7 (48 hpf; P=0.4 versus wild type). We interpreted these data to indicate that *eya4* deficiency did not promote cell death.

Because *eya4* is also expressed in neuromasts of the lateral line sensory system (Schonberger et al., 2005), we assessed neuromast hair cells labeled with the vital dye DASPEI (Whitfield et al., 1996). At 72 hpf, wild-type zebrafish (n=13) had 10-17 neuromasts on the lateral line sensory system of each flank, and each neuromast contained approximately five hair cells (Fig. 5A,C). By contrast, *eya4* morphant fish (MO3eya4, n=6; MO10eya4, n=7) had fewer than six neuromasts along the lateral line sensory system of each flank, and each neuromast contained only one or two hair cells (MO3eya4, $P=2\times10^{-21}$; MO10eya4, $P=5\times10^{-29}$; Fig. 5B,C). Neither MO3mis (n=4 fish) nor MO10mis (n=6 fish) altered the total number of neuromasts or the hair cell numbers per neuromast (P=0.11, MO3mis versus wild type; Fig. 5C).

Sensory function in *eya4* morphant fish

The otic vesicle and the lateral line sensory system are required for a normal startle reflex in zebrafish, or a 'tail-flip' escape response that is elicited by clicks, tapping or vibrational stimuli (Whitfield et al., 2002). Wild-type zebrafish exhibit this response by 72 hpf, and swim with coordinated movements away from startle stimuli (see Movie 3 in the supplementary material). We assessed the individual responses of 80 wild-type and morphant fish (72 hpf; see Table S1 in the supplementary material). All 80 wild type and 25 *eya4* morphant fish had normal startle reflexes. However, 70% (n=55) of the *eya4* morphant fish had abnormal startle reflexes ($P=2.1\times10^{-23}$) and swam with un-coordinated movements in small circles (see Movie 4 in the supplementary material). Normal startle responses were preserved in MO3mis- or MO10mis-treated fish (n>100 morphant fish; data not shown).

Altered *atp1b2b* expression in *eya4*-deficient zebrafish

Six Na^+/K^+-ATPase subunits are expressed in the zebrafish otic vesicle early in embryogenesis (Blasiole et al., 2003): *atp1b2b*, *atp1a1a.1*, *atp1a1a.2*, *atp1a1a.4*, *atp1a1a.5* and *atp1b1a*. Five of these genes have developmental expression patterns in the otic vesicle that differ from *eya4* expression patterns, whereas the temporal and spatial expression pattern of *atp1b2b* (Blasiole et al., 2003) mirrored *eya4* expression (24 and 72 hpf). Hypothesizing that *eya4* might regulate expression of this β2b subunit of Na^+/K^+-ATPase, we first confirmed *atp1b2b* expression in the otic vesicle

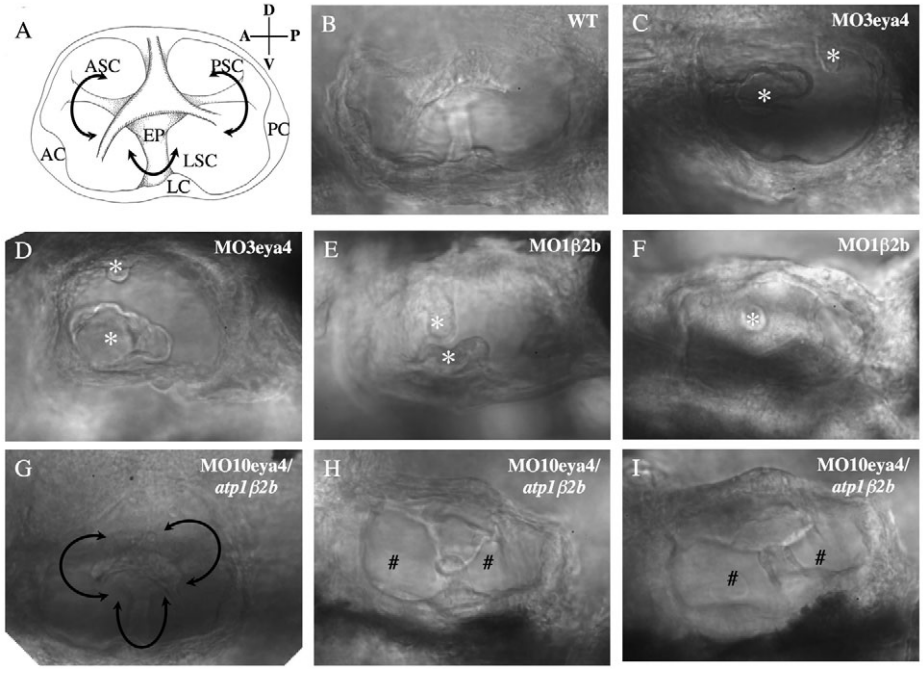

Fig. 3. Otic vesicle morphology in wild-type and morphant fish (72 hpf). (**A**) Schematic of the normal otic vesicle structures visualized by differential interference contrast (DIC) imaging. Anterior, lateral and posterior cristae (AC, LC and PC, respectively) have differentiated into anterior, lateral and posterior semicircular canals (ASC, LSC and PSC, respectively) that are portioned by epithelial pillars (EP) inside the otic vesicle. (**B**) DIC image of the otic vesicle in wild-type fish reveals normal structures. (**C**,**D**) DIC images of otic vesicles from *eya4* morphant fish show aborted protrusions of presumptive epithelial pillars (asterisks) into the vesicle and malformed canals. (**E**,**F**) DIC images of *atp1b2b* morphant fish otic vesicles show incomplete fusion and diminutive epithelial pillars (asterisks), which resemble those of the *eya4* morphants. (**G-I**) *atp1b2b* mRNA-rescued *eya4* morphant fish otic vesicles were still smaller than wild type, but were larger than *eya4* morphant vesicles. Canal formation was partially (# in H,I) or nearly completely restored (G) as a result of the more mature epithelial pillars.

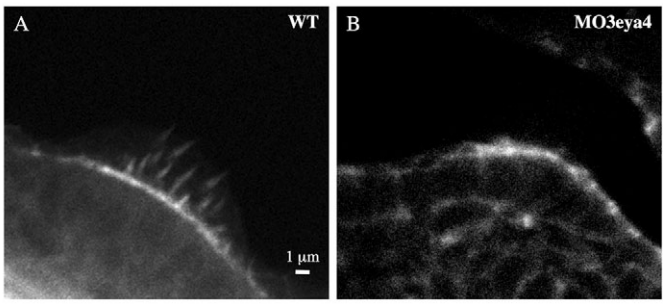

Fig. 4. Compromised hair cell development *eya4* morphant fish. (**A**) At 72 hpf the ampulla of the posterior cristae of wild-type fish (n=10) have delicate hair cell stereocilia (stained with FITC-labeled phalloidin) that appear as spikes. (**B**) Stereocilia in hair cells of *eya4* morphant fish (n=12) are dysmorphic and reduced in number.

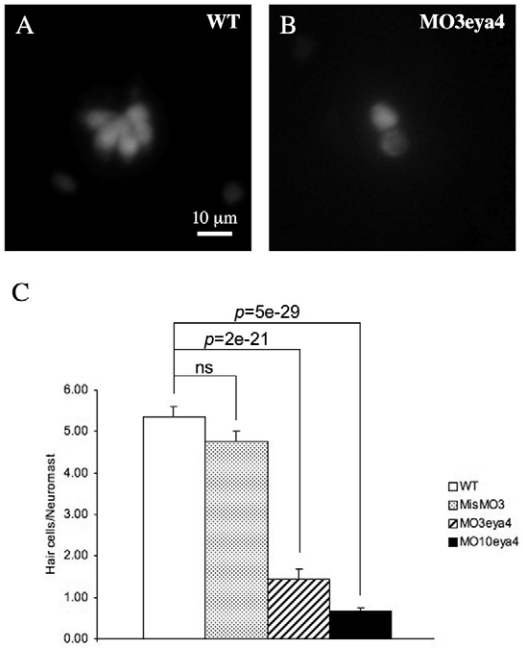

Fig. 5. Reduced numbers of neuromast hair cells in *eya4* morphant fish. Wild-type (**A**) and *eya4* morphant (**B**) fish were stained with DASPEI, and neuromast hair cells were imaged and counted (**C**).

by whole-mount in situ hybridization (72 hpf). We also identified *atp1b2b* expression in the lateral line neuromasts, as well as in the retina and somites (Fig. 6A,B,D). Expression of *atp1b2b* in the heart was low and was detected only by section in situ hybridization, with ventricular expression of *atp1b2b* exceeding atrial expression (Fig. 6D). To independently validate cardiac *atp1b2b* expression, the plasmid pβ2bprom (containing a 2.5-kb promoter fragment of *atp1b2b* upstream of *EGFP*) was injected into zebrafish embryos. Cardiac fluorescence was detected at 48 hpf and 72 hpf (Fig. 6E, data not shown), therein confirming *atp1b2b* expression in the heart.

eya4 morpholinos reduced *atp1b2b* expression

Levels of *atp1b2b* mRNA (assessed by semi-quantitative RT-PCR) in *eya4* morphant fish were approximately 50% of wild-type levels (Fig. 6F). Levels of *atp1a1a.1*, *atp1a1a.2*, *atp1a1a.4* and *atp1b1a* mRNAs were comparable in *eya4* morphant fish and wild-type fish (Fig. 6F). Although the *atp1a1a.5* mRNA level was also reduced (Fig. 6F) in *eya4* morphant fish, further studies did not focus on this gene because of the different spatial pattern of expression of *atp1a1a.5* (Blasiole et al., 2003) and *eya4* (Fig. 1).

eya4 morphant *atp1b2b* expression was assessed by whole-mount in situ hybridization. Wild type and *eya4* morphant *atp1b2b* expression was similar in the retina, somite, pectoral fin and mature neuromasts (data not shown). However, *atp1b2b* signal was notably missing or reduced in the sensory epithelium of the malformed *eya4* morphant otic vesicle (compare Fig. 6B with 6C).

Attenuated *atp1b2b* expression recapitulates *eya4* morphant phenotypes

If *eya4* regulation of *atp1b2b* expression contributed to the observed developmental defects, we reasoned that attenuated expression of this Na^+/K^+-ATPase subunit would mimic the otic vesicular, neuromast and cardiac phenotypes found in *eya4* morphant fish. Two antisense morpholino oligonucleotides directed against splice donor sites at the junction of exon 1-intron 1 (MO1β2b) and exon 4-intron 4 (MO4β2b) of the *atp1b2b* gene were constructed and studied (Fig. 7). RT-PCR and sequencing analysis confirmed abnormal *atp1b2b* splicing (data not shown), resulting in the deletion of 346 nucleotides and excision of the translation initiation site by MO1β2b, and the deletion of 32 nucleotides, which produced a frameshift in exon 4, by MO4β2b.

Zebrafish injected with MO1β2b (n=42) or MO4β2b (n=70) had significantly reduced *atp1b2b* expression (data not shown) and indistinguishable phenotypes. *atp1b2b* morphant fish demonstrated diminutive, malformed otic vesicles and under-developed semicircular canals resembling the anatomical defects found in *eya4* morphant fish (Fig. 2, Fig. 3E,F). In addition, about 43% of *atp1b2b* morphant fish lacked one or both otoliths, whereas wild-type fish and all *eya4* morphant fish had two normally developed otoliths (Fig. 7A-C). The sensory cristae in 25 *atp1b2b* morphant fish contained an average of three to four hair cells per cristae (comparable to the average of <3 hair cells per cristae in *eya4* morphants). Among the 27 *atp1b2b* morphants in which neuromast hair cells were identified (Fig. 7D), there were significantly fewer hair cells than in wild-type neuromasts (P=0.001).

Acridine Orange staining was used to assess cell death in the *atp1b2b* morphants at 24 and 48 hpf (see Fig. S2 in the supplementary material). Only background level staining was observed at both stages (24 hpf, average number of stained cells=0.1±0.3 per otic vesicle, n=16 fish, P=0.3 versus wild type; 48 hpf, average number of stained cells=0.2±0.5 per otic vesicle, n=20 fish, P=0.4 versus wild type; Fig. S2 in the supplementary material), indicating that hair cell death was not increased in *atp1b2b* morphant fish.

Startle responses (see Movie 5 in the supplementary material) were abnormal in more than 85% (n=61) of *atp1b2b* morphant fish ($P=7.2\times10^{-11}$ versus wild type). In 52 *atp1b2b* morphant fish, startle responses were completely absent, while two morphant fish had uncoordinated movements similar to that observed in *eya4* morphant fish.

Cardiac phenotypes in *atp1b2b* morphant fish also recapitulated those in *eya4* morphant fish (n=9): ventricular chambers were smaller than wild-type hearts (P=0.05 versus wild-type systolic diameter; P=0.004 versus wild-type diastolic diameter) and pericardial effusions were present in 77% (99 of 128) *atp1b2b* morphant fish (Fig. 7B,C,E). Heart rates were also significantly slower (P=0.003) in *atp1b2b* morphants (n=9) than in wild-type fish (Fig. 7E) or *eya4* morphant fish, which have heart rates comparable to wild type (Schonberger et al., 2005).

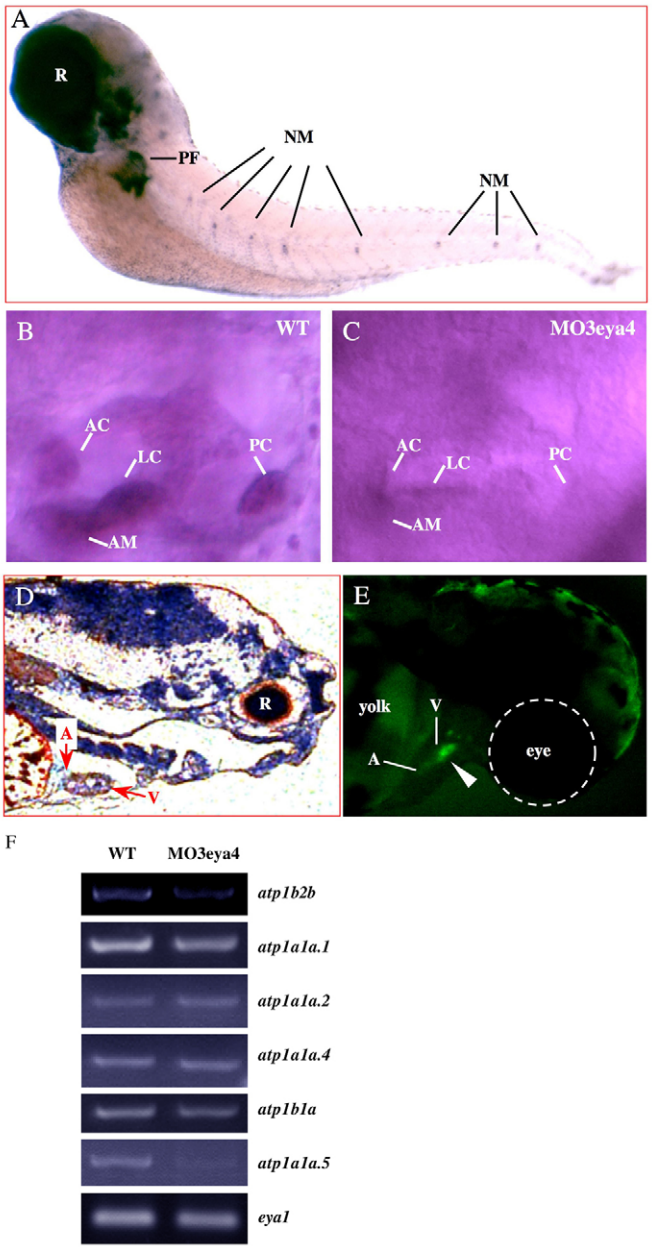

Fig. 6. *atp1b2b* expression in zebrafish embryos (72 hpf). (**A**) Whole-mount in situ hybridization with DIG-labeled *atp1b2b* antisense probe revealed expression in the otic vesicle, neuromast (NM), retina (R) and pectoral fin (PF). (**B**) Higher resolution image of *atp1b2b* expression in a lateral view of the otic vesicle with robust signals in the anterior macula (AM), and the anterior, lateral and posterior cristae (AC, LC and PC, respectively) in wild type. (**C**) In the *eya4* morphant otic vesicle, *atp1b2b* expression was notably reduced in the AC, LC, PC and AM. (**D**) In situ hybridization of sections using a radiolabeled *atp1b2b* antisense probe show *atp1b2b* expression in the heart. Expression in the ventricle (V) is greater than in the atrium (A). DIG and radiolabeled *atp1b2b* sense probes produced low background signals (data not shown). (**E**) Fluorescent signal (arrowhead) detected at 72 hpf in zebrafish injected with plasmid pβ2bprom confirmed *atp1b2b* promoter activity and EGFP expression. (**F**) Semi-quantitative RT-PCR (see Materials and methods) showed reduced *atp1b2b* expression in *eya4* morphant fish compared with wild type. MO3eya4 did not alter *eya1* expression (Schonberger et al., 2005). Semi-quantitative RT-PCR on other Na^+/K^+-ATPase subunits that were expressed in the otic vesicle, including *atp1a1a.1*, *atp1a1a.2*, *atp1a1a.4*, *atp1b1a* and *atp1a1a.5*, are also shown.

atp1b2b is regulated by *eya4* in zebrafish during otic vesicle and cardiac development

We reasoned that if *eya4* regulated *atp1b2b* (either directly or indirectly), then *eya4-atp1b2b* double morphants should replicate and perhaps accentuate the phenotypes of either an *eya4* or *atp1b2b* single morphant. By contrast, if these molecules functioned in independent developmental pathways, much more severe phenotypes would be expected in the double morphants than in either of the single morphant fish.

Lower doses of *eya4* and *atp1b2b* morpholino oligonucleotides than those previously used (so as to minimize non-specific morpholino toxicity and to minimize the potential for lethal heart failure) were co-injected into embryos and resultant phenotypes were assessed. Dose titration of MO3eya4 and MO1β2b indicated that fish injected with either 0.5 ng of MO3eya4 or 1.8 ng of MO1β2b were viable and developed 12-15 neuromasts on each flank (n>9), with significantly reduced (average=3) hair cells per neuromast (MO3eya4, $P=2\times10^{-6}$ versus wild type; MO1β2b, $P=7\times10^{-6}$ versus wild type). Normal hair cell numbers (six or seven per cristae) were observed in the mono-morphant otic vesicles (MO3eya4, n=22; MO1β2b, n=15; P=not significant; see Table S1 in the supplementary material). In fish (n=76) treated with MO1β2b (1.8 ng), seven morphants lacked one otolith and one morphant lacked both otoliths. Small pericardial effusions were found in mono-morphant fish (MO3eya4, n=31; MO1β2b, n=60), and only one MO1β2b mono-morphant demonstrated severe heart failure (versus 77% observed with a higher MO1β2b dose).

Embryos co-injected with both 0.5 ng of MO3eya4 and 1.8 ng of MO1β2b had hair cell numbers that were not significantly different from fish injected with identical doses of single morpholinos. Double-morphant embryos had 12-16 neuromasts on each flank with an average of three hair cells per neuromast (n=13, P=0.66 versus MO3eya4 and P=0.68 versus MO1β2b) and an average of six to seven hair cells per cristae, (n=17, P=not significant; see Table S1 in the supplementary material). Of 64 double morphants, two lacked one otolith and one lacked both otoliths. Only three double morphants showed severe heart failure.

Because the double-morphant studies supported the model that *eya4* regulated *atp1b2b*, we determined whether overexpression of *atp1b2b* mRNA could rescue phenotypes produced by *eya4* deficiency. Embryos injected with in vitro transcribed *atp1b2b* mRNA (50-70 pg) showed no malformations (data not shown). Embryos were therefore co-injected with MO10eya4 and 70 pg *atp1b2b* mRNA, and otic vesicle morphology, cardiac function and startle reflexes were characterized (Table 1).

Otic vesicle formation was markedly improved in fish (72 hpf) co-injected with MO10eya4 and *atp1b2b* mRNA. Unlike the severely malformed otic vesicle in *eya4* morphant fish, approximately 50% of co-injected fish had otic vesicles that were smaller but otherwise indistinguishable from those of wild-type fish. Notably, the development of epithelial pillars and the formation of semicircular canals was rescued (Fig. 3G-I). Co-injected fish had normal numbers of sensory hair cells in the otic vesicle (n=5) and neuromasts (n=17) that were not significantly different from wild-type fish (Table 1). Startle responses in co-injected fish were also improved: 83% (103/123) of fish treated with MO10eya4 and *atp1b2b* mRNA had normal swimming patterns (see Movie 6 in the supplementary material; Table 1).

Cardiac structure and function was also improved in fish co-injected with MO10eya4 and *atp1b2b* mRNA (Fig. 8A,B). Atrial and ventricular sizes were normal and pericardial effusions were

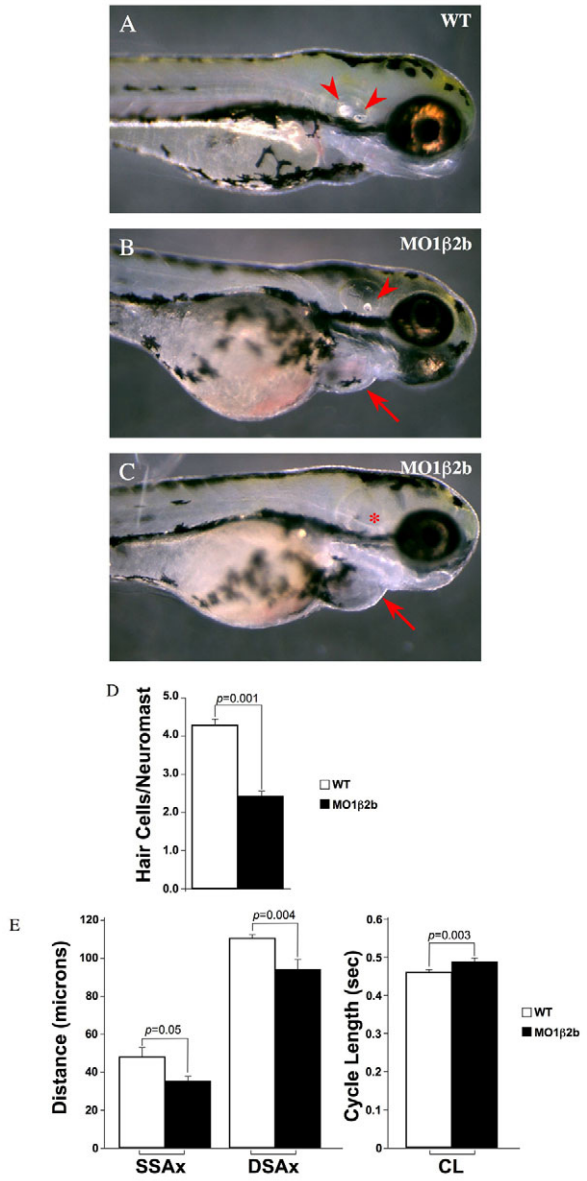

Fig. 7. Phenotypes of *atp1b2b* morphant fish (72 hpf). (**A**) Otic vesicles from wild-type embryos contained two otoliths (arrowheads). (**B**,**C**) *atp1b2b* morphant fish lacked one (B) or both (asterisk, C) otoliths and had ventral protuberances due to pericardial effusion (arrows), consistent with cardiac failure. (**D**) *atp1b2b* morphant neuromasts had significantly fewer hair cells than wild-type embryos. (**E**) Cardiac ventricular chamber sizes were smaller and contractile cycle length was longer (corresponding to slower heart rate) in *atp1b2b* morphant fish compared with wild-type fish. SSAx, systolic short axis; DSAx, diastolic short axis; CL, cycle length.

completely absent in 59% (72/123) of co-injected embryos, whereas only 5% (5 out of 80) of *eya4* morphant fish had normal heart structure (P=1.8×10^{-8}; Table 1).

DISCUSSION

We report an essential role for *eya4* expression in the development of the zebrafish otic vesicle sensory epithelia and neuromasts. Eya4 deficiency attenuated hair cell numbers, disrupted maturation of the otic vesicle and perturbed normal sensory responses. We suggest

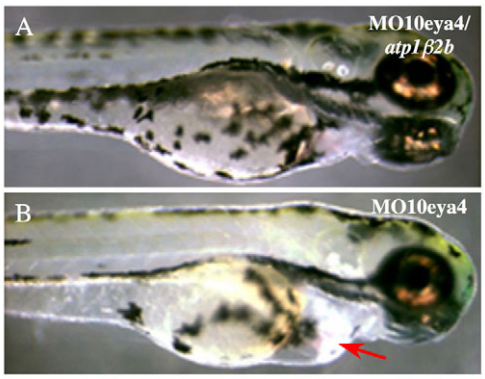

Fig. 8. *atp1b2b* mRNA rescued *eya4* morphant phenotypes. (**A**,**B**) The hearts of *atp1b2b* mRNA-rescued *eya4* morphant fish (A) lacked pericardial effusion, visible in *eya4* morphant fish (arrow, B).

that the *atp1b2b* gene is a direct or indirect downstream target of Eya4 – a conclusion based on the colocalized temporal and spatial expressions of *eya4* and *atp1b2b*, the diminished *atp1b2b* expression in *eya4* morphant fish, and the similar phenotypes found in zebrafish treated with either *atp1b2b* or *eya4* antisense morpholino oligonucleotides. Moreover, *eya4-atp1b2b* double morpholino oligonucleotides did not demonstrate a synergistic effect and overexpression of atp1*b2b* mRNA partially compensated for *eya4* deficiency, restoring both sensory hair cells, and cardiac development and function.

There is substantial evidence that Eya proteins are important for auditory system development in multiple vertebrate species. Human *EYA4* mutations cause sensorineural hearing loss either in isolation or with cardiomyopathy; *EYA1* mutations cause Branchio-Oto-Renal syndrome (BOR) with sensorineural hearing loss, craniofacial and kidney defects (Abdelhak et al., 1997), phenotypes that are largely recapitulated in *Eya1*-deficient mice (Xu et al., 1999). In zebrafish, *eya1* gene mutations cause the *dog-eared* phenotype (Whitfield et al., 1996), which is characterized by small otic vesicles, malformed semicircular canals, reduced numbers of hair cells in the otic vesicle and the lateral line neuromasts, and diminutive jaw structure (Kozlowski et al., 2005). The otic vesicle and neuromast malformations are remarkably similar to those found in *eya4* morphant fish, a result that we interpreted to indicate participation by *eya1* and *eya4* in a common regulatory network during development of the zebrafish sensory system. However, the broader pattern of *eya1* expression, diffusely throughout the ventral part of the otic vesicle at 24 hpf (Sahly et al., 1999), in contrast to the restricted focal *eya4* expression in regions that will form the sensory epithelium, implied that each of these molecules had specific roles in otic vesicle development. In support of these distinct functions, we note that unlike *eya1*-deficient animals, *eya4* morphants did not show ectopic cell death in the developing otic vesicle. Selective functions by these transcriptional co-activators is further evident from their distinct extra-sensory phenotypes that involve the heart (*eya4*) (Schonberger et al., 2005) or mandible (*eya1*) (Kozlowski et al., 2005).

Eya proteins do not bind DNA directly, but require both Six and Dachshund transcription factors to mediate regulatory effects. Because the zebrafish genome encodes 10 *six* genes (Bessarab et al., 2004; Kobayashi et al., 2000; Seo et al., 1999; Seo et al., 1998a; Seo et al., 1998b), identification of the specific Six proteins that interact with Eya4 has been problematic. Two gene family members, *six1*

Table 1. Phenotypes of wild type, *eya4* morphants, and *eya4* morphants rescued with *atp1b2b* RNA

				Statistical comparisons (*P*) between *atp1b2b* rescue	
	Wild type	*eya4* morphant*	*atp1b2b* rescue	Versus wild type	Versus *eya4* morphant
Number of fish	80	80	123		
Abnormal startle response	0 (0%)	55 (68.7%)	20 (16.3%)	0.0004	2.9×10^{-14}
Abnormal cardiac morphology	0 (0%)	75 (93.7%)	51 (41.5%)	5.4×10^{-12}	1.8×10^{-8}
Number of fish	10	12	5		
Hair cells/anterior cristae	7.0±0.6	1.7±0.7	5.8±2.0	0.60	0.017
Hair cells/lateral cristae	5.0±0.4	1.4±0.6	4.3±0.9	0.56	0.035
Hair cells/posterior cristae	4.1±0.5	1.3±0.4	5.2±1.3	0.48	0.001
Number of fish	13	6	17		
Hair cells/neuromast	5.4±0.2	1.5±0.2	3.9±0.4	0.21	5.3×10^{-11}

**eya4* morphant fish were studied at 72 hpf.
atp1b2b rescue denotes co-injection of the *eya4* morpholino oligonucleotide and *atp1b2b* RNA, studied at 72 hpf.
Statistical comparisons are between *atp1b2b*-rescued fish and wild type, or between *atp1b2b*-rescued fish and *eya4* morphant fish.

and *six4.1*, are expressed in the zebrafish otic vesicle (Bessarab et al., 2004; Kobayashi et al., 2000), but neither has an expression pattern that matches that of *eya4*. At 24 hpf, *six1* is diffusely expressed in the ventral edge of the otic vesicle and expression decreases subsequently (Bessarab et al., 2004); *six4.1* is expressed in the maculae and the vestibular/acoustic ganglia at 37 hpf (Bessarab et al., 2004; Kobayashi et al., 2000). *six4.1* is also weakly expressed in the semicircular canals (at 60 hpf) (Bessarab et al., 2004; Kobayashi et al., 2000), but not within the cristae where *eya4* expression localizes.

Because insufficient information about Eya4-binding partners hindered the identification of target genes, we selected candidate genes for study. Because Na^+/K^+-ATPase has important roles in hearing and cardiac physiology, organ systems perturbed by human *EYA4* mutations, zebrafish genes encoding α and β subunits were evaluated. Six of fifteen Na^+/K^+-ATPase α and β subunit genes are expressed in the zebrafish otic vesicle (Blasiole et al., 2003), but only two, *atp1b2b* and *atp1a1a.5*, had altered RNA levels in *eya4* morphant fish (Fig. 6). The expression pattern of *atp1a1a.5* was distinct from that of *eya4*. At 24 hpf, *atp1a1a.5* expression was found diffusely within the anteroventral portion of the otic vesicle, whereas *eya4* expression was punctuate (Fig. 1A). Later in development, *atp1a1a.5* is found in the dorsolateral septum and the anterior, posterior and lateral semicircular pillars (Blasiole et al., 2003), regions that do not express *eya4*. Taken together, we concluded that *eya4* regulation of *atp1a1a.5* occurred in tissues other than the otic vesicle. By contrast, *atp1b2b* expression colocalized with *eya4*, and, based on previous studies indicating that *atp1b2b* deficiency delayed development of the semicircular canal (Blasiole et al., 2006), we concluded that *eya4* regulated *atp1b2b* during otic vesicle development.

This model was supported by shared phenotypes in *eya4* and *atp1b2b* morphant fish: attenuated hair cell development in otic vesicles and neuromasts, and malformations of the semicircular canals. Consistent with these data, *atp1b2b* morphant fish, like *eya4* morphant fish, had sensory function abnormalities (see Movie 5 in the supplementary material). In addition, the phenotypes in *eya4-atp1b2b* double morphants resembled those of *eya4* and *atp1b2b* mono-morphants. To corroborate that *eya4* and *atp1b2b* function in a shared developmental pathway, we performed studies that paralleled the rescue experiments of *atp1a1a.1*-deficient zebrafish by exogenous zebrafish *atp1a1a.1* mRNA or rat *Atp1a1* mRNA (Blasiole et al., 2006), and assessed whether exogenous *atp1b2b* could rescue *eya4* morphant fish. Because of zebrafish *atp1b2b* is only 65% identical to its mammalian homolog *Atp1b2*, we overexpressed zebrafish *atp1b2b* in *eya4* morphant fish and found both the cardiac and sensory system phenotypes were rescued (Fig. 8, Table 1). Taken together, we concluded that *atp1b2b* is a direct or indirect target of *eya4*.

We noted a correlation (Table 1, Fig. 4A; see also Table S1 in the supplementary material; $r>0.4$ for all two-way comparisons) between the numbers of hair cells in different otic vesicle cristae and the anterior macula of *eya4* morphant fish (data not shown), but whether this correlation reflects independent or related developmental processes is unclear. Perhaps *eya4* is essential for development of the primordial cells that give rise to sensory hair cells throughout the otic placode, a model that is supported by expression early in development (14 hpf; see Fig. S1A in the supplementary material). Alternatively, *eya4* expression could be required for independent processes that occur in the maculae and cristae and impact on hair cell development.

The diminutive size of the otic vesicle in *eya4* and *atp1b2b* morphant fish, as well as the maldeveloped epithelium pillars and semicircular canals (Figs 2, 3), implicate roles for *eya4* beyond development of the sensory epithelium. That broad consequences would result from the disruption of *eya4*, a transcriptional co-activator that probably regulates many genes, was not entirely unexpected. However, that multiple structural defects arose because of the dysregulation of a Na^+/K^+-ATPase subunit indicates that the ionic milieu is crucial for multiple aspects of otic vesicle development.

In situ hybridization experiments and a reporter assay also demonstrated *atp1b2b* expression in the embryonic zebrafish heart (Fig. 6D,E). Three other Na^+/K^+-ATPase subunit genes are expressed in the zebrafish heart: *atp1a1a.1*, *atp1a2* and *atp1b1a* (Cheng et al., 2003; Shu et al., 2003; Yuan and Joseph, 2004). Whereas *atp1a2* is believed to regulate cardiac laterality (Shu et al., 2003), the function of *atp1b1a* remains elusive (Cheng et al., 2003). *Heart and mind* and *small heart* phenotypes (diminutive hearts with slow beating rates) result from *atp1a1a.1* mutations (Shu et al., 2003; Yuan and Joseph, 2004). *atp1b2b* morphant fish also had small hearts and slower beating rates, raising the possibility that *atp1b2b* interacts with the *atp1a1a.1* subunit in the heart. This subunit pairing has also been suggested to be important for otic vesicle development (Blasiole et al., 2006). Although the function of Na^+/K^+-ATPase in cardiac biology remains incompletely understood, we suggest that human *EYA4* mutations affect the heart in part by altering the expression of Na^+/K^+-ATPase.

Some *atp1b2b* morphant fish had two additional phenotypes that were not observed in *eya4* morphant fish. Most *atp1b2b* morphant fish lacked either one or both otoliths (Fig. 7B,C), whereas otolith

agenesis was never observed in *eya4* morphant fish. Previous studies (Blasiole et al., 2006) of *atp1b2b* morphant fish reported the presence of at least one otolith, a difference that may reflect the selective efficacy of *atp1b2b* morpholino oligonucleotides that targeted splicing (this report) or translation initiation. In addition, a slower heart rate was observed in the *atp1b2b* morphant fish (Fig. 7E) but not in the *eya4* morphant fish (Schonberger et al., 2005). Although other explanations are possible, we suggest that the additional phenotypes in *atp1b2b* morphant fish are due to a considerably greater (>90%) reduction in *atp1b2b* mRNAs than is seen in *eya4* morphants (50% reduction of *atp1b2b* mRNAs).

We are intrigued by the observation that zebrafish Eya4 regulates the same Na^+/K^+-ATPase subunit in both the heart and the hair cell in the sensory system. In humans, EYA4-deficiency impacts both of these organs, raising the possibility that the regulation of Na^+/K^+-ATPase subunits in mammals has been conserved throughout evolution. Despite the improved phenotypes in *eya4* morphant fish produced by *atp1b2b* mRNA, we expect that other genes expressed in these tissues are also regulated by *eya4*. Further understanding of the composition of Eya4-Six-Dach complexes and their DNA recognition sites should yield more insights into the regulatory pathways influenced by Eya4 that account for human sensorineural hearing loss and dilated cardiomyopathy.

We greatly appreciate the scientific comments from David A. Conner and his critical reading of the manuscript. We are grateful to Jost Schönberger for his valuable discussions. We thank José Rivera-Feliciano, Jenna Galloway, Sarah Keller, Haobing Wang, Yariv Houvras, Bruce Barut and Susanne Bartlett for their technical assistance. This work was supported by grants from the Howard Hughes Medical Institute (C.E.S.) and the National Institutes of Health (J.G.S. and C.E.S.).

Supplementary material

Supplementary material for this article is available at
http://dev.biologists.org/cgi/content/full/135/20/3425/DC1

References

Abdelhak, S., Kalatzis, V., Heilig, R., Compain, S., Samson, D., Vincent, C., Weil, D., Cruaud, C., Sahly, I., Leibovici, M. et al. (1997). A human homologue of the Drosophila eyes absent gene underlies branchio-oto-renal (BOR) syndrome and identifies a novel gene family. *Nat. Genet.* **15**, 157-164.

Ausubel, F., Brent, R., Kingston, R. E., Moore, D. D., Seidman, J. G., Smith, J. A. and Struhl, K. (2008). *Current Protocols in Molecular Biology.* New York, NY: John Wiley and Sons.

Bessarab, D. A., Chong, S. W. and Korzh, V. (2004). Expression of zebrafish six1 during sensory organ development and myogenesis. *Dev. Dyn.* **230**, 781-786.

Blanco, G. and Mercer, R. W. (1998). Isozymes of the Na-K-ATPase: heterogeneity in structure, diversity in function. *Am. J. Physiol.* **275**, F633-F650.

Blasiole, B., Canfield, V., Degrave, A., Thisse, C., Thisse, B., Rajarao, J. and Levenson, R. (2002). Cloning, mapping, and developmental expression of a sixth zebrafish Na,K-ATPase alpha1 subunit gene (atp1a1a.5). *Gene Expr. Patterns* **2**, 243-246.

Blasiole, B., Degrave, A., Canfield, V., Boehmler, W., Thisse, C., Thisse, B., Mohideen, M. A. and Levenson, R. (2003). Differential expression of Na,K-ATPase alpha and beta subunit genes in the developing zebrafish inner ear. *Dev. Dyn.* **228**, 386-392.

Blasiole, B., Canfield, V. A., Vollrath, M. A., Huss, D., Mohideen, M. A., Dickman, J. D., Cheng, K. C., Fekete, D. M. and Levenson, R. (2006). Separate Na,K-ATPase genes are required for otolith formation and semicircular canal development in zebrafish. *Dev. Biol.* **294**, 148-160.

Cheng, K. C., Levenson, R. and Robishaw, J. D. (2003). Functional genomic dissection of multimeric protein families in zebrafish. *Dev. Dyn.* **228**, 555-567.

Goldin, S. M. (1977). Active transport of sodium and potassium ions by the sodium and potassium ion-activated adenosine triphosphatase from renal medulla. Reconstitution of the purified enzyme into a well defined in vitro transport system. *J. Biol. Chem.* **252**, 5630-5642.

Hanson, I. M. (2001). Mammalian homologues of the Drosophila eye specification genes. *Semin. Cell Dev. Biol.* **12**, 475-484.

Horowitz, B., Eakle, K. A., Scheiner-Bobis, G., Randolph, G. R., Chen, C. Y., Hitzeman, R. A. and Farley, R. A. (1990). Synthesis and assembly of functional mammalian Na,K-ATPase in yeast. *J. Biol. Chem.* **265**, 4189-4192.

Ingwall, J. S. and Balschi, J. A. (2006). Energetics of the Na(+) pump in the heart. *J. Cardiovasc. Electrophysiol.* **17 Suppl 1**, S127-S133.

Jorgensen, P. L. (1974). Purification and characterization of (Na+ plus K+)-ATPase. IV. Estimation of the purity and of the molecular weight and polypeptide content per enzyme unit in preparations from the outer medulla of rabbit kidney. *Biochim. Biophys. Acta* **356**, 53-67.

Jowett, T. (1999). Analysis of protein and gene expression. *Methods Cell Biol.* **59**, 63-85.

Kawakami, K., Sato, S., Ozaki, H. and Ikeda, K. (2000). Six family genes-structure and function as transcription factors and their roles in development. *BioEssays* **22**, 616-626.

Kobayashi, M., Osanai, H., Kawakami, K. and Yamamoto, M. (2000). Expression of three zebrafish Six4 genes in the cranial sensory placodes and the developing somites. *Mech. Dev.* **98**, 151-155.

Kozlowski, D. J., Whitfield, T. T., Hukriede, N. A., Lam, W. K. and Weinberg, E. S. (2005). The zebrafish dog-eared mutation disrupts eya1, a gene required for cell survival and differentiation in the inner ear and lateral line. *Dev. Biol.* **277**, 27-41.

Levenson, R. (1994). Isoforms of the Na,K-ATPase: family members in search of function. *Rev. Physiol. Biochem. Pharmacol.* **123**, 1-45.

Li, X., Oghi, K. A., Zhang, J., Krones, A., Bush, K. T., Glass, C. K., Nigam, S. K., Aggarwal, A. K., Maas, R., Rose, D. W. et al. (2003). Eya protein phosphatase activity regulates Six1-Dach-Eya transcriptional effects in mammalian organogenesis. *Nature* **426**, 247-254.

Malik, N., Canfield, V., Sanchez-Watts, G., Watts, A. G., Scherer, S., Beatty, B. G., Gros, P. and Levenson, R. (1998). Structural organization and chromosomal localization of the human Na,K-ATPase beta 3 subunit gene and pseudogene. *Mamm. Genome* **9**, 136-143.

Peters, T. A., Kuijpers, W. and Curfs, J. H. (2001). Occurrence of NaK-ATPase isoforms during rat inner ear development and functional implications. *Eur. Arch. Otorhinolaryngol.* **258**, 67-73.

Pfister, M., Toth, T., Thiele, H., Haack, B., Blin, N., Zenner, H. P., Sziklai, I., Nurnberg, P. and Kupka, S. (2002). A 4-bp insertion in the eya-homologous region (eyaHR) of EYA4 causes hearing impairment in a Hungarian family linked to DFNA10. *Mol. Med.* **8**, 607-611.

Rajarao, S. J., Canfield, V. A., Mohideen, M. A., Yan, Y. L., Postlethwait, J. H., Cheng, K. C. and Levenson, R. (2001). The repertoire of Na,K-ATPase alpha and beta subunit genes expressed in the zebrafish, Danio rerio. *Genome Res.* **11**, 1211-1220.

Rajarao, J. R., Canfield, V. A., Loppin, B., Thisse, B., Thisse, C., Yan, Y. L., Postlethwait, J. H. and Levenson, R. (2002). Two Na,K-ATPase beta 2 subunit isoforms are differentially expressed within the central nervous system and sensory organs during zebrafish embryogenesis. *Dev. Dyn.* **223**, 254-261.

Rayapureddi, J. P., Kattamuri, C., Steinmetz, B. D., Frankfort, B. J., Ostrin, E. J., Mardon, G. and Hegde, R. S. (2003). Eyes absent represents a class of protein tyrosine phosphatases. *Nature* **426**, 295-298.

Rebay, I., Silver, S. J. and Tootle, T. L. (2005). New vision from Eyes absent: transcription factors as enzymes. *Trends Genet.* **21**, 163-171.

Sahly, I., Andermann, P. and Petit, C. (1999). The zebrafish eya1 gene and its expression pattern during embryogenesis. *Dev. Genes Evol.* **209**, 399-410.

Schonberger, J., Levy, H., Grunig, E., Sangwatanaroj, S., Fatkin, D., MacRae, C., Stacker, H., Halpin, C., Eavey, R., Philbin, E. F. et al. (2000). Dilated cardiomyopathy and sensorineural hearing loss: a heritable syndrome that maps to 6q23-24. *Circulation* **101**, 1812-1818.

Schonberger, J., Wang, L., Shin, J. T., Kim, S. D., Depreux, F. F., Zhu, H., Zon, L., Pizard, A., Kim, J. B., Macrae, C. A. et al. (2005). Mutation in the transcriptional coactivator EYA4 causes dilated cardiomyopathy and sensorineural hearing loss. *Nat. Genet.* **37**, 418-422.

Schwinger, R. H., Bundgaard, H., Muller-Ehmsen, J. and Kjeldsen, K. (2003). The Na, K-ATPase in the failing human heart. *Cardiovasc. Res.* **57**, 913-920.

Seo, H. C., Drivenes Ellingsen, S. and Fjose, A. (1998a). Expression of two zebrafish homologues of the murine Six3 gene demarcates the initial eye primordia. *Mech. Dev.* **73**, 45-57.

Seo, H. C., Drivenes, O., Ellingsen, S. and Fjose, A. (1998b). Transient expression of a novel Six3-related zebrafish gene during gastrulation and eye formation. *Gene* **216**, 39-46.

Seo, H. C., Curtiss, J., Mlodzik, M. and Fjose, A. (1999). Six class homeobox genes in Drosophila belong to three distinct families and are involved in head development. *Mech. Dev.* **83**, 127-139.

Shamraj, O. I. and Lingrel, J. B. (1994). A putative fourth Na+,K(+)-ATPase alpha-subunit gene is expressed in testis. *Proc. Natl. Acad. Sci. USA* **91**, 12952-12956.

Shu, X., Cheng, K., Patel, N., Chen, F., Joseph, E., Tsai, H. J. and Chen, J. N. (2003). Na,K-ATPase is essential for embryonic heart development in the zebrafish. *Development* **130**, 6165-6173.

Therien, A. G. and Blostein, R. (2000). Mechanisms of sodium pump regulation. *Am. J. Physiol. Cell Physiol.* **279**, C541-C566.

Tootle, T. L., Silver, S. J., Davies, E. L., Newman, V., Latek, R. R., Mills, I. A., Selengut, J. D., Parlikar, B. E. and Rebay, I. (2003). The transcription factor Eyes absent is a protein tyrosine phosphatase. *Nature* **426**, 299-302.

Underhill, D. A., Canfield, V. A., Dahl, J. P., Gros, P. and Levenson, R. (1999). The Na,K-ATPase alpha4 gene (Atp1a4) encodes a ouabain-resistant alpha

subunit and is tightly linked to the alpha2 gene (Atp1a2) on mouse chromosome 1. *Biochemistry* **38**, 14746-14751.
Wangemann, P. (2002). K+ cycling and the endocochlear potential. *Hear Res.* **165**, 1-9.
Wayne, S., Robertson, N. G., DeClau, F., Chen, N., Verhoeven, K., Prasad, S., Tranebjarg, L., Morton, C. C., Ryan, A. F., Van Camp, G. et al. (2001). Mutations in the transcriptional activator EYA4 cause late-onset deafness at the DFNA10 locus. *Hum. Mol. Genet.* **10**, 195-200.
Westerfield, M. (2000). *The Zebrafish Book: A Guide for the Laboratory Use of Zebrafish (*Danio rerio*)*. Eugene, OR: University of Oregon Press.
Whitfield, T. T. (2002). Zebrafish as a model for hearing and deafness. *J. Neurobiol.* **53**, 157-171.
Whitfield, T. T., Granato, M., van Eeden, F. J., Schach, U., Brand, M., Furutani-Seiki, M., Haffter, P., Hammerschmidt, M., Heisenberg, C. P., Jiang, Y. J. et al. (1996). Mutations affecting development of the zebrafish inner ear and lateral line. *Development* **123**, 241-254.
Whitfield, T. T., Riley, B. B., Chiang, M. Y. and Phillips, B. (2002). Development of the zebrafish inner ear. *Dev. Dyn.* **223**, 427-458.
Xu, P. X., Adams, J., Peters, H., Brown, M. C., Heaney, S. and Maas, R. (1999). Eya1-deficient mice lack ears and kidneys and show abnormal apoptosis of organ primordia. *Nat. Genet.* **23**, 113-117.
Yuan, S. and Joseph, E. M. (2004). The small heart mutation reveals novel roles of Na+/K+-ATPase in maintaining ventricular cardiomyocyte morphology and viability in zebrafish. *Circ. Res.* **95**, 595-603.